Adsorption of Xanthene Dyes by Lysozyme Crystals

Aleksandar Cvetkovic,† Adrie J. J. Straathof,*,† Rajamani Krishna,‡ and Luuk A. M. van der Wielen†

Department of Biotechnology, Delft University of Technology, Julianalaan 67, 2628 BC Delft, The Netherlands, and Van 't Hoff Institute for Molecular Sciences, University of Amsterdam, Nieuwe Achtergracht 166, 1018 WV Amsterdam, The Netherlands

Received September 1, 2004. In Final Form: November 9, 2004

Adsorption characteristics of cross-linked lysozyme crystals of different morphologies (tetragonal, orthorhombic, triclinic and monoclinic) were examined using four anionic dyes (fluorescein, eosin, erythrosin, and rose bengal), one zwitterionic dye (rhodamine B), and one cationic dye (rhodamine 6G). The adsorption isotherms were of the Langmuir type for all examined systems with the exception of rhodamine B adsorption by monoclinic crystals. The weakest adsorption was observed for the cationic dye, rhodamine B, whereas dianionic dyes, eosin, rose bengal, and erythrosin were strongly adsorbed on the protein surface. The adsorption capacities of the crystals for the dyes were found to depend on both charge and hydrophobicity of the dye, reflecting the heterogeneous character of the lysozyme pore surface. The adsorption affinity of the crystals for the dyes was a function of the dyes' hydrophobicity. Furthermore, the crystal morphology was identified as an additional factor determining capacity and affinity for dye adsorption. Differences between crystals prepared in the presence of the same precipitant were lower than between morphologies prepared with different precipitants.

Introduction

In the development of protein-containing catalytic and separation materials, proteins are normally immobilized on the surface of inert matrixes. An increasingly large number of researchers are claiming that crystalline forms of enzyme and other proteins have substantial advantages over lyophilized powders and proteins immobilized on surfaces.[1−3] The wide variety of molecular topologies found in protein crystals makes them a novel class of nanoporous materials.[4] However, they have not been widely exploited in the past, apart from their use in the determination of protein structures. This is due to their nature, which is inherently fragile and prone to dissolution even under benign conditions. Developments in cross-linking technology have provided crystals with sufficient stability, enabling their routine use in a broad range of fields, including biocatalysis,[1,5] medical formulations and detergent applications,[1] and separation processes such as chromatography.[4,6]

Despite the significant potential of cross-linked protein crystals (CLPCs) in industrial applications, understanding of their fundamental properties is still in its infancy, especially in the area of adsorption. Studies on the hydration and dehydration of lysozyme crystals[7] and on the electrophoretic mobility of NaCl, $NaNO_3$, and NaSCN adsorbed by tetragonal lysozyme crystals from aqueous solutions[8] did not provide deeper understanding of the adsorption processes. Recently, however, a study on fluorescein adsorption on cross-linked and native lysozyme crystals identified the type and the concentration of cosolute, solution pH, and intensity of cross-linking as parameters determining solute adsorption.[9] Although a better insight into the mechanisms behind solute adsorption by lysozyme crystals was obtained, several topics were left unaddressed, namely, the influence of the crystal structure and of the type of the solute. The aim of the present study is address these topics by determining the nature of solute−solute and solute−protein interactions during solute adsorption by protein crystals of different morphologies from single-component adsorption experiments.

A family of xanthene dyes—rose bengal, eosin, erythrosin, fluorescein, rhodamine B, and rhodamine 6G (Figure 1)—with varying charges and hydrophobicities will be used to adsorb on cross-linked tetragonal lysozyme crystals. These dyes are model solutes, which can diffuse into the crystal.[10] In addition, adsorption of two dyes, namely, rhodamine B and fluorescein, by crystals of four different morphologies (tetragonal, orthorhombic, triclinic, and monoclinic) will be presented.

Materials and Methods

Materials. Chicken egg white lysozyme was obtained from Sigma (product no. L-6876; 95% purity; M = 14307 g/mol) and was used without further purification. Four different structures of lysozyme crystals were grown and cross-linked according to the procedure described in Cvetkovic et al.[9]

Disodium salts of fluorescein (Sigma, product no. F-6377), eosin (Sigma, product no. E4382), erythrosin (Fluka product no.45690),

* To whom correspondence may be addressed. E-mail: A.J.J.Straathof@tnw.tudelft.nl. Phone: +31-15-2782330. Fax: +31-15-2782355.

† Delft University of Technology.

‡ University of Amsterdam.

(1) Margolin, A. L.; Navia, M. A. *Angew. Chem., Int. Ed.* **2001**, *40*, 2205−2222.

(2) Jen, A.; Merkle, H. P. *Pharmaceut. Res.* **2002**, *18*, 1483−1488.

(3) Shenoy, B.; Wang, Y.; Shan, W. Z.; Margolin, A. L. *Biotechnol. Bioeng.* **2001**, *73*, 358−369.

(4) Vilenchik, L. Z.; Griffith, J. P.; St Clair, N.; Navia, M. A.; Margolin, A. L. *J. Am. Chem. Soc.* **1998**, *120*, 4290−4294.

(5) St Clair, N. L.; Navia, M. A. *J. Am. Chem. Soc.* **1992**, *114*, 7314−7316.

(6) Pastinen, O.; Jokela, J.; Eerikainen, T.; Schwabe, T.; Leisola, M. *Enzyme Microb. Technol.* **2000**, *26*, 550−558.

(7) Gevorkyan, S. G.; Morozov, V. N. *Biofizika* **1983**, *28*, 1002−1007.

(8) Lee, H. M.; Kim, Y. W.; Baird, J. K. *J. Cryst. Growth* **2001**, *232*, 294−300.

(9) Cvetkovic, A.; Zomerdijk, M.; Straathof, A. J. J.; Krishna, R.; van der Wielen, L. A. M. *Biotechol. Bioeng.* **2004**, *87*, 658−668.

(10) Cvetkovic, A.; Straathof, A. J. J.; Hanlon, D. N.; van der Zwaag, S.; Krishna, R.; van der Wielen, L. A. M. *Biotechnol. Bioeng.* **2004**, *86*, 389−398.

10.1021/la0478090 CCC: $30.25
Published on Web 01/20/2005

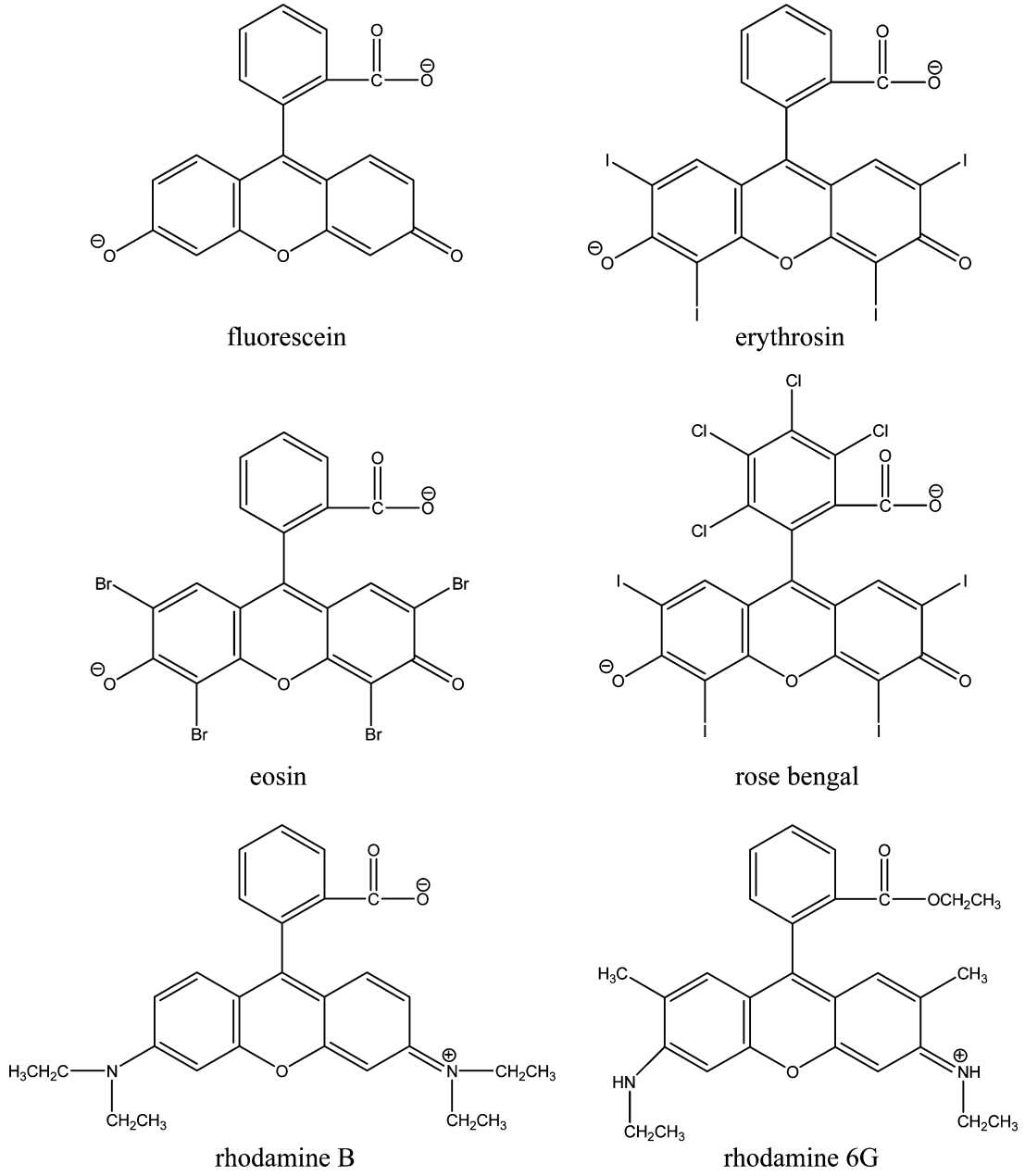

Figure 1. Chemical structure of dyes used in this study.

and rose bengal (Fluka product no. 11950), hydrochloride of rhodamine B (Fluka product no. 83690), and chloride salt of rhodamine 6G (Fluka product no. 83697) were used as a fluorescent dyes.

Evaluation of Adsorption Properties for Dye−Crystal Systems. The cross-linked crystals were filtered and washed with deionized water using 0.45 μm membrane filters (Supor-200, Gelman Laboratory). Different amounts of the wet (filtered) crystals were accurately weighed and suspended in vials with 2.00 mL or in tubes with 15 or 45 mL of aqueous solution, containing a dye in a concentration of 26 μmol·L^{-1}. The suspensions were stored in tightly sealed vials or tubes wrapped in aluminum foil to prevent degradation by light. To determine the time needed to reach equilibrium, independent sets of dynamic uptake experiments were performed for every dye used in this study and for cross-linked tetragonal crystals in a stirred vessel of 100 mL. Samples of 1.0 mL were taken every 5 min in the beginning of the experiments and then every 2 h, until equilibrium was reached. Equilibrium in the dynamic uptake experiment was reached after 2−10 days, and there was no swelling of the crystals according to our previous study.[9] Therefore, for the other experiments, suspensions were equilibrated at room temperature with a constant shaking, and after 14−20 days the mixture was centrifuged.

Dye concentrations in the supernatant solution were determined using a UV−visible spectrophotometer (Pharmacia, Ultrospec III) at their adsorption maxima of 544, 524, 516, 490, 556, and 526 nm for rose bengal, erythrosin, eosin, fluorescein, rhodamine B, and rhodamine 6G, respectively.

The results were then used to determine adsorbate loading on the lysozyme crystals with a mass balance

$$(C_j^{L,0} - C_j^{L})V^{L} = (q_j - q_j^{0})m^{cr} \quad (1)$$

$C^{L,0}$ and C^{L} are initial and final dye (j) concentrations (mol L^{-1}) in the bulk liquid, respectively, q^0 and q are initial and final dye concentrations (mol kg^{-1}) in the solid phase, respectively, and m^{cr} is the mass (kg) of the wet crystals calculated as described elsewhere.[9] The initial solid-phase concentration is zero.

Processing of Adsorption Data. Considering the fact that fluorescein adsorption by lysozyme crystals can be described by the Langmuir adsorption model,[9] a rearranged form of the

Table 1. Physical and Adsorption Characteristics and Process Parameters for the Dye Adsorption by Cross-Linked Tetragonal Crystals (Initial Concentration of the Dye Solutions Was 25.9 μmol·L^{-1})

	M/ (g·mol^{-1})	log· ($K_{oct-wat}$)[a]	charge at exp conditions	pH_0	pH_{end}	b/ (10^4 L·mol^{-1})	R_L/(10^3)	Q_{sat}/ (10^{-2} mol·kg^{-1})	Q_{sat}/ (mol·mol^{-1})[h]	K/(10^3)
Rose Bengal	971.7	11.36	dianion[c]	7.26	6.2−7.1	106.6 ± 16.7	35 ± 5	6.80 ± 0.07	0.476 ± 0.005	90.0 ± 13.1
Erythrosin	833.9	8.52	dianion[d]	7.62	6.4−6.9	95.0 ± 17.0	39 ± 6	8.40 ± 0.12	0.588 ± 0.009	99.2 ± 16.1
Eosin	645.9	7.48	dianion[e]	6.89	6.3−7.2	54.7 ± 2.4	66 ± 3	10.24 ± 0.09	0.727 ± 0.006	69.6 ± 2.43
Fluorescein	330.8	4.05	dianion/monoanion[f]	6.14	6.3−6.9	19.6 ± 0.6	165 ± 4	6.39 ± 0.06	0.447 ± 0.005	15.6 ± 0.27
Rhodamine B	442.6	5.54	zwitterion[g]	7.18	6.3−7.2	3.02 ± 0.06	561 ± 5	1.78 ± 0.02	0.124 ± 0.002	0.667 ± 0.00
Rhodamine 6G	442.6	5.8[b]	cation	6.81	5.7−6.2	34.7 ± 0.4	100 ± 1	0.58 ± 0.00	0.040 ± 0.000	2.48 ± 0.02

[a] From Egbaria and Friedman: Egbaria, K.; Friedman, M. *Pharmaceut. Res.* **1992**, *9*, 629−635. [b] Calculated using the Hansch substituent effect.[12] [c] From Amat-Guerri et al.: Amat-Guerri, F.; Lopez-Gonzalez, M. M. C.; Sastre, R.; Martinez-Utrilla, R. *Dyes Pigm.* **1990**, *13*, 219−232. [d] From Mchedlov-Petrossyan: Mchedlov-Petrossyan, N. O. *Zh. Org. Khim.* **1983**, *19*, 797−805. [e] From Mchedlov-Petrossyan and Kukhtik: Mchedlov-Petrossyan, N. O.; Kukhtik, V. I. *Dyes Pigm.* **1994**, *24*, 11−35. [f] From Sjoback et al.: Sjoback, R.; Nygren, J.; Kubista, M. *Spectrochim. Acta, Part A* **1995**, *51*, L7-L21. [g] From Arbeloa and Ojeda: Arbeloa, I. L.; Ojeda, P. R. *Chem. Phys. Lett.* **1981**, *79*, 347−350. [h] Moles of dye per mole of lysozyme in crystal.

Langmuir equation was used in this study to analyze the adsorption of dyes on the cross-linked lysozyme crystals

$$\frac{C_j^{\mathrm{L}}}{q_j} = \frac{1}{b_j Q_{\mathrm{sat},j}} + \frac{1}{Q_{\mathrm{sat},j}} C_j^{\mathrm{L}} \tag{2}$$

where b_j and $Q_{\mathrm{sat},j}$ are constants indicating affinity (L mol^{-1}) and capacity (mol kg^{-1}), respectively, of the crystal for the dye j. If the Langmuir equation is obeyed, a plot of C_j^{L}/q_j versus C_j^{L} should yield a straight line with a slope of $1/Q_{\mathrm{sat},j}$ and with an intercept of $1/(b_j Q_{\mathrm{sat},j})$.

A further analysis of the Langmuir equation can be made on the basis of a dimensionless separation parameter, R_{L},[11] also known as the separation factor given by

$$R_{\mathrm{L}} = \frac{1}{1 + b_j C_j^{\mathrm{L},0}} \tag{3}$$

R_{L} shows that adsorption is favorable if $0 < R_{\mathrm{L}} < 1$, unfavorable if $R_{\mathrm{L}} > 1$, irreversible if $R_{\mathrm{L}} = 0$, and linear if $R_{\mathrm{L}} = 1$.[11] In the case of a linear adsorption isotherm, eq 2 can be simplified

$$\frac{q_j}{C_j^{\mathrm{L}}} = Q_{\mathrm{sat},j} b_j = \rho^{\mathrm{cr}} K_j \tag{4}$$

K represents the linear distribution coefficient of dye in the system and ρ^{cr} is the crystal density in kg m^{-3}.

Results

Cross-Linked Tetragonal Crystals: Influence of the Solute. During adsorption experiments, the final pH of the dye solutions was generally between pH 6 and 7 as observed previously for fluorescein.[9] This is caused by the buffering effect of the lysozyme, and hence the pH shift is not only dependent on the buffering capacity of the dye solution but also on the amount of crystals (Table 1). Within a series of experiments, slightly different final pH values were observed.

Figure 2 illustrates the equilibrium isotherms (i.e. q versus C^{L}) for six different xanthene dyes by cross-linked tetragonal crystals. Adsorption isotherms were of Langmuirian type as presented in Figure 3. Table 1 lists the Langmuir parameters b and Q_{sat}, solute distribution coefficients between the phases (K), and separation factors (R_{L}) calculated using eqs 2−4, in addition to physicochemical properties of the xanthene dyes. The capacity of cross-linked tetragonal crystals varied from 5.8 to 103.2 mmol·kg^{-1}, which corresponds to 0.040−0.717 dye/lysozyme mole ratio. The other Langmuir coefficient, the affinity, related to the dye−crystal equilibrium has values in the range of 30−1066 L·mmol^{-1}, which indicates

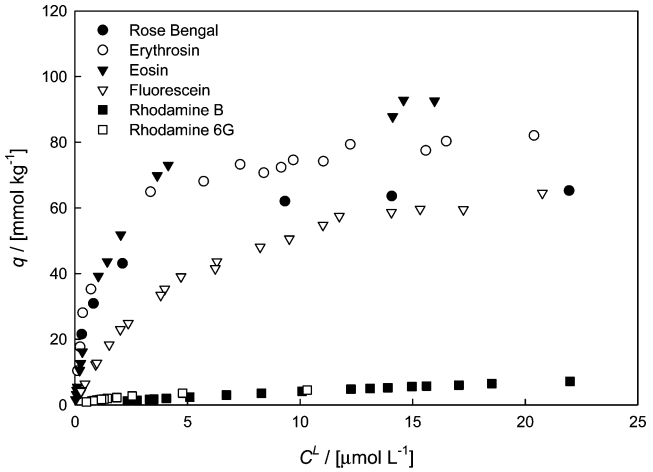

Figure 2. Adsorption of the xanthene dyes by cross-linked tetragonal lysozyme crystals. Starting concentration of dyes in the solutions was 26 μmol·L^{-1}. For experimental details see Table 1.

that not only capacities but also binding forces are widely different for different solutes. The values of the separation factor showed that adsorption by tetragonal lysozyme crystals was favorable and might be exploited for practical applications.

Two separate sets of curves can be observed in Figure 3. For anionic xanthenes (rose bengal, erythrosin, eosin, and fluorescein) higher saturation levels than those for rhodamine B and rhodamine 6G are found. At the experimental pH, rhodamine B is zwitterionic and rhodamine 6G is cationic (Figure 1 and Table 1). The capacity of cross-linked tetragonal crystals for negatively charged dyes was 4−20 times higher than those for the other two dyes and the affinity was 1- to 2-fold higher (Table 1).

Crystal Morphology. Proteins can be crystallized in different crystal forms, depending on the type and concentration of the precipitant and the buffer, on the concentration of the protein, on temperature, and on pH. Type and position of the protein−protein interactions will be determined by the crystallization conditions and this can lead to differences in solute adsorption. Adsorption of fluorescein and rhodamine B on four lysozyme crystal morphologies was studied, and the results are presented in Figure 4. The isotherms were of the Langmuir type for all systems studied except for the rhodamine B−monoclinic crystal system for which a linear isotherm was found in the experimental concentration range.

Adsorption characteristics depend on the crystal structure in addition to the solute characteristics as shown in Figure 4. Such a relationship was not established previ-

(11) Hall, K. R.; Eagleton, L. C.; Acrivos, A.; Vermeule, T. *Ind. Eng. Chem. Fundam.* **1966**, *5*, 212−222.

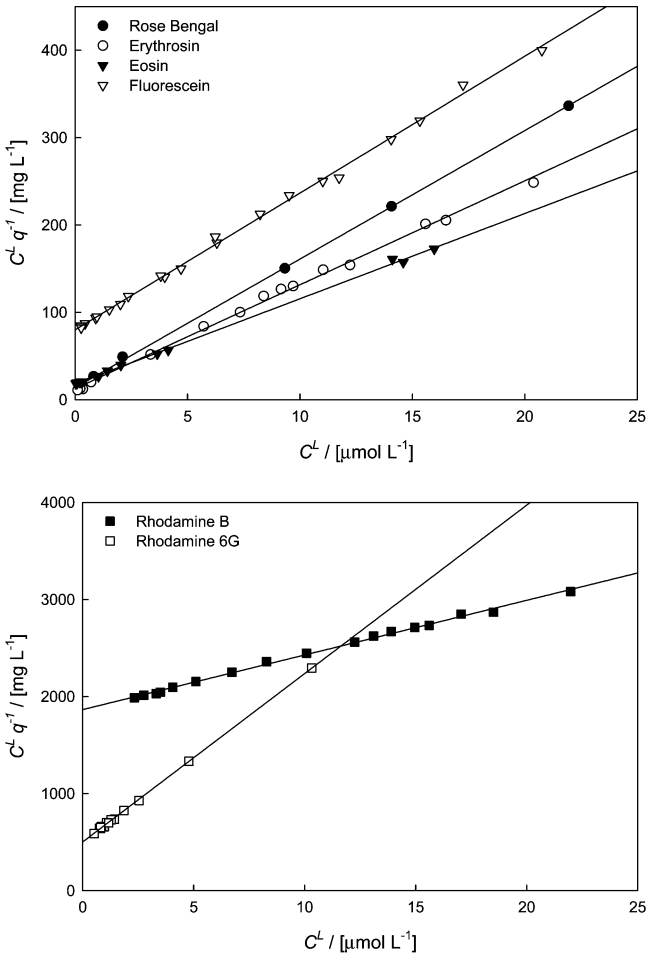

Figure 3. Adsorption of xanthene dyes by cross-linked tetragonal lysozyme crystals. Markers are experimental data, and lines are linear regression fits by eq 2.

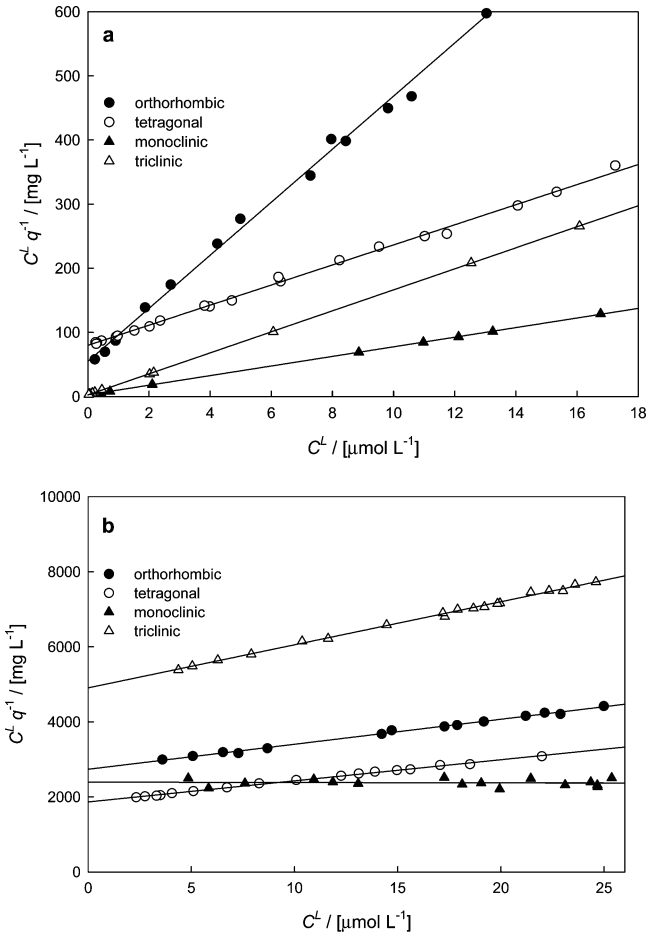

Figure 4. Adsorption of (a) fluorescein and (b) rhodamine B by cross-linked lysozyme crystals of all available crystal structures. Markers are experimental data and lines are linear regression fits of eq 2.

ously because in the published experiments the pH of the solution was an interfering factor.[9] The fluorescein capacity varied from 23 to 134 mmol·kg^{-1} for the orthorhombic and monoclinic crystal morphology, respectively, and the affinity varied in the range from 200 to 6450 L·mmol^{-1} (Table 2). The values of the separation factor showed that fluorescein adsorptions by the tetragonal and orthorhombic morphologies were favorable and those by the monoclinic and tetragonal morphologies were practically irreversible.

In the case of rhodamine B, the observed capacity and affinity were in the range of 8.7−17.8 mmol·kg^{-1} and 23−30 L·mmol^{-1}, respectively. Separation factors were favorable and almost identical (0.56−0.62) for the experimental systems studied with the exception of the rhodamine B−monoclinic crystals system, for which a linear isotherm was found in the experimental concentration range.

Discussion

Fluorescein probes of varying charge and hydrophobicities were used to study solute protein interactions in the aqueous suspension of cross-linked crystals. As will be discussed, hydrophobicities and charges of solutes and protein, solute and pore size, pore surface state, and counteranions of protein in the crystal may determine the adsorption of solute by protein crystals.

Electrostatic Interactions. It was established that electrostatic interactions play an important role in the adsorption of xanthene dyes by tetragonal lysozyme crystals (Figures 2 and 3). Considering that lysozyme was positively charged at the experimental conditions (pK_i = 11.2), the capacity for the dyes depends on the protonation state of the dyes and decreases in the following order: dianions (rose bengal, erythrosin, and eosin), mixture of mono- and dianions (fluorescein), zwitterions (rhodamine B), and cations (rhodamine 6G). However, such a correlation was not observed for the affinity. Moreover, the differences between the dianions (Table 1) could not be explained on the basis of electrostatic interactions.

The same correlation could be observed for other crystal morphologies used in the study (Table 2) where distribution coefficient, affinity, and capacity of the crystals, regardless of crystal morphology, were higher for fluorescein than for rhodamine B and distribution coefficients for the different crystal morphologies were negatively correlated for fluorescein and rhodamine B (Table 2).

Hydrophobic Interactions. Incorporation of halogen in the fluorescein molecules increases their hydrophobicity. This hydrophobicity might be responsible for the changes of affinities in Table 1. A positive correlation between a solute's hydrophobicity, quantified here as the logarithm of the dyes' partitioning coefficient between octanol and water (one of the several possible ways of representation),[12] and the affinity of the tetragonal crystals for the dyes was established (Table 1) when five dyes were considered (Figure 5). The exception was rhodamine B. Unfortunately, for the dyes used in this study, hydrophobicity is correlated to the molar mass (Table 1), so a

(12) Leo, A.; Hansch, C.; Elkins, D. *Chem. Rev.* **1971**, *71*, 525−616.

Table 2. Langmuir Adsorption Parameters after Rhodamine B and Fluorescein Uptake from Their Solution with Initial Concentration of 26 μmol·L^{-1} by Cross-Linked Lysozyme Crystals

		fluorescein at $pH_0 = 6.14$						rhodamine B at $pH_0 = 7.18$					
crystal morphology	ϵ (%)	pH_{end}	$b/(10^4$ L·mol$^{-1})$	$R_L/(10^3)$	$Q_{sat}/$ (10^{-2} mol·kg^{-1})	$Q_{sat}/$ (mol·mol$^{-1})^a$	$K/(10^3)$	pH_{end}	$b/(10^4$ L·mol$^{-1})$	$R_L/(10^3)$	$Q_{sat}/$ (10^{-2} mol·kg^{-1})	$Q_{sat}/$ (mol·mol$^{-1})^a$	K
orthorhombic	46	6.0–7.0	79.3 ± 9.3	46 ± 5	2.31 ± 0.03	0.163 ± 0.002	23.8 ± 2.5	5.7–6.5	2.44 ± 0.06	613 ± 6	1.50 ± 0.03	0.106 ± 0.002	477 ± 4
tetragonal	44	6.5–7.0	19.6 ± 0.6	164 ± 4	6.39 ± 0.06	0.469 ± 0.005	15.6 ± 0.3	6.3–7.2	3.02 ± 0.06	561 ± 5	1.78 ± 0.02	0.130 ± 0.002	665 ± 3
monoclinic	38	6.4–7.0	279.7 ± 26.8	14 ± 1	13.36 ± 0.04	1.121 ± 0.004	462.9 ± 42.6	6.0–6.7	<3.83[b]	100 ± 0	>1.09[b]	>0.080[b]	523 ± 14
triclinic	36	6.1–7.4	645.0 ± 63.5	6 ± 1	6.10 ± 0.01	0.496 ± 0.001	499.2 ± 48.4	5.6–6.7	2.34 ± 0.04	622 ± 4	0.87 ± 0.01	0.071 ± 0.001	259 ± 1

[a] Mole of dye per mole of lysozyme in crystal. [b] Saturation was not observed in the experiments; interval is based on the highest q observed.

Figure 5. Affinity of the solute to crystal as a function of solute's hydrophobicity.

similar correlation as in Figure 5 would be observed if molar mass was used instead hydrophobicity (data not shown). Capacity, which correlated to the solutes' protonation state as mentioned before, was correlated inversely with hydrophobicity of these dianionic dyes (Table 1).

Steric Interactions. If we assume that the solute size is proportional to the cube root of the molar mass of the dyes and porosity is proportional to the average pore size (for simplicity we neglect the fact that actual pore sizes may be widely different from the average), the crystal with the smaller porosity will have the smaller average pore size and the solutes with smaller molar mass will have a smaller solute size. There was no correlation between the size of the solute and capacity for the solutes (Table 1). Also, the porosity did not correlate with the capacity (Table 2). However, a positive correlation was established between the solute size and affinity (Table 1). This was not anticipated considering steric interactions and may be the result of the aforementioned hydrophobic interactions.

A decrease of porosity did not change the affinity for rhodamine B, but the affinity for fluorescein seemed to be increasing (Table 2). However, since this increase was observed only for fluorescein, it probably does not originate from the pore size but from other interactions.

Influence of Pore Surface State and Protein Counteranion. The pore structure is not isotropic in protein crystals;[10] therefore the adsorption will be determined by the real pore structure. The characteristics of the pore surface (position of the residues) are determined by protein–protein bonds established during crystallization. Many of these bonds can only be established in the presence of ions (anions in the case of lysozyme) provided to the crystallization solution in the form of precipitant salts. The number and position of counterions varies for different crystal morphologies and can even vary for one crystal morphology depending on the used precipitant. For example, the monoclinic crystal has 6 nitrate or 16 iodide ions per lysozyme molecule in its structure.[13] This may influence the level of the electrostatic interactions in the system and, with it, the adsorption of the solute. In this study, protein counterions were nitrate for the monoclinic and triclinic morphology (six per lysozyme) and chloride for the tetragonal and orthorhombic morphology (one per lysozyme). Conversely, four out of six

(13) Steinrauf, L. K. *Acta Crystallogr., Sect. D: Biol. Crystallogr.* **1998**, *54*, 767–779.

nitrates are in the same position in monoclinic and triclinic lysozyme crystal structure[14] which may explain their similar adsorption behavior (Table 2). The same conclusions can be drawn for orthorhombic and tetragonal morphologies. On the contrary, large differences were found for the morphologies with different protein counterions in their crystal structure.

Even if there is a similarity in the adsorption behavior between morphologies with the same protein counterions in their crystal structure, the behavior is not identical—one morphology has a higher affinity than the other morphology and vice versa for their capacities (Table 2). This can be a result of the differences in pore size but also of differences in the pore surface state. For example, arginine side-chain conformations in orthorhombic and tetragonal forms[15] differ by around 50%, as a result of participation of the arginine residues in protein interactions that will lead to the diverse adsorption behavior.

The results show a potentially interesting ability of protein crystals to concentrate, collect, and store solutes from a surrounding solution. Thus, protein crystals can find applications as biocompatible carriers of drugs and other active substances. A drawback might be diffusion limitation due to their small pore sizes.[10] Therefore, the use of nanocrystals may be a solution.[16] Note that the usage of specific crystal morphology will depend on the characteristics of the solute (charge, hydrophobicity, and size) and protein characteristics can be adjusted to obtain the best separation.

Conclusions

Our study demonstrates that adsorption of solutes by protein crystals depend simultaneously on several parameters including solute, protein, and crystal characteristics. Electrostatic and hydrophobic interactions have been identified as the main sources of xanthene dye adsorption on lysozyme protein crystals. Additionally, adsorption is determined by the crystal structure of the protein, probably due to differences between the protein counterions in the crystals.

Acknowledgment. The Netherlands Organisation for Scientific Research—Chemical Sciences (NWO-CW) has funded this work. We thank Max Zomerdijk for his help in initial experimental work.

LA0478090

(14) Walsh, M. A.; Schneider, T. R.; Sieker, L. C.; Dauter, Z.; Lamzin, V. S.; Wilson, K. S. *Acta Crystallogr., Sect. D*: *Biol. Crystallogr.* **1998**, *54*, 522−546.

(15) Oki, H.; Matsuura, Y.; Komatsu, H.; Chernov, A. A. *Acta Crystallogr., Sect. D*: *Biol. Crystallogr.* **1999**, *55*, 114−121.

(16) Martin, R. W.; Zilm, K. W. *J. Magn. Reson.* **2003**, *165*, 162−174.